Age-Related Accumulation and Spatial Distribution of Lipofuscin in RPE of Normal Subjects

François C. Delori,[1,2] *Douglas G. Goger,*[1] *and C. Kathleen Dorey*[1,2,3]

Purpose. To characterize the age-related accumulation of lipofuscin in a population of normal subjects, resolve differences in estimated accumulation rates obtained in previous studies, and characterize the spatial distribution of lipofuscin in the normal fundus.

Methods. Spectrophotometric measurements were made at the fovea and 7° temporal to the fovea in 145 normal subjects (age range, 15–80 years). Spatial distribution along the four cardinal meridians was measured in selected subjects by both spectrophotometry and autofluorescence imaging. To minimize contributions of extraneous fluorophores, macular pigment, and melanin, all measurements used excitation at 550 nm, integrating emission between 650 and 750 nm.

Results. Lipofuscin fluorescence increased linearly until age 70, then declined. The rate of accumulation was significantly slower in the fovea than at the temporal site; accumulation rates in vivo were greater than previously observed in microscopic studies. Fluorescence was ~40% lower in the fovea than at 7° eccentricity and was asymmetrically distributed around the fovea. The fluorescence was maximal at ≈11° temporally, ≈7° nasally, ≈13° superiorly, and ≈9° inferiorly. At the same eccentricity, fluorescence was always less along the inferior meridian than along any other.

Conclusions. Light absorption by RPE melanin can explain differences between the in vivo and ex vivo estimates of the rate of lipofuscin accumulation. Declining fluorescence at old age may represent removal of atrophic RPE cells. The spatial distribution of lipofuscin generally matches that of rods and reflects, rather than predicts, the pattern of age-related loss of rod photoreceptors. (*Invest Ophthalmol Vis Sci.* 2001;42: 1855–1866)

In the human retinal pigment epithelium (RPE), lipofuscin accumulates as a byproduct of phagocytosis of photoreceptor outer segments. Over age 70, lipofuscin and melanolipofuscin granules may occupy as much as 20% to 33% of the free cytoplasmic space of the cell.[1] It has been postulated that excessive levels of lipofuscin could compromise essential RPE functions and/or contribute to the pathogenesis of age-related macular degeneration (AMD).[1–5] The spatial topography, age-relationship, and racial distributions of lipofuscin exhibit remarkable similarity to patterns seen in AMD (summarized by Dorey et al.[6]). The concept that excessive lipofuscin may be harmful is supported by the observation that regions of geographic atrophy in eyes with AMD were often surrounded by bands of elevated lipofuscin fluorescence.[7]

The association between lipofuscin accumulation and retinal degeneration is most clearly delineated in Stargardt's macular dystrophy, an inherited retinal degeneration characterized by high levels of lipofuscin,[8] and caused by defects in the ABCR gene (Rim protein)[9,10] expressed specifically in rods and cones.[11] Lipofuscin levels in patients with Stargardt's macular dystrophy were found to be significantly higher than those in normal subjects of the same age.[12,13] Excessive lipofuscin accumulation preceded photoreceptor loss in mice carrying null mutations in the ABCR gene.[14] Furthermore, loss of visual function in other inherited retinal degenerations such as vitelliform macular dystrophy (Best's disease)[15] and Batten's disease (ceroid-lipofuscinosis)[16] has also been attributed to excessive accumulation of lipofuscin-like materials in lysosomes of the RPE.

Lipofuscin is potentially noxious, for it acts as a photosensitizer in blue light, generating free radicals both in isolated granules[17,18] and within the RPE cell.[19] Lipofuscin contains several distinct fluorescent components,[20] one of which is A2E, a pyridinium bisretinoid.[21,22] The precursor of A2E is formed in the photoreceptor from sequential reactions of phosphatidylethanolamine and two molecules of vitamin A; subsequent hydrolysis releases A2E.[23,24] This red-emitting fluorophore of lipofuscin also has noxious effects on RPE cells in vitro: it inhibits lysosomal digestion of proteins,[25] and causes blue-light–mediated disruption of lysosomal membranes[26] and RPE apoptosis.[27] Lipofuscin colocalizes with lysosomal enzymes in neurons,[28,29] and exogenous A2E is delivered to lysosomes of RPE cells in vitro.[30] If released into the cytoplasm, A2E selectively attacks mitochondria and releases cytochrome C and AIF (apoptosis-inducing factor), which initiate apoptosis.[31] Subsequent removal of apoptopic RPE could explain the reduced levels of lipofuscin observed in eyes with advanced Best's disease[32] and AMD.[6,33]

To probe the relationship between lipofuscin accumulation and photoreceptor loss with age, and in macular degenerations, we and others developed spectrophotometric and imaging techniques to study lipofuscin fluorescence in vivo.[34–36] Using spectrophotometry,[37] we have demonstrated that the spectrum of the dominant fundus fluorophore is consistent with that of chloroform extracts of lipofuscin-laden human RPE cells[4] and with that of the lipofuscin fluorophore VIII identified by Eldred and Katz[20] and subsequently shown to be A2E.[21,22] Additionally, the spectrum of elevated fluorescence in patients with Stargardt's disease corresponds with that in normal subjects.[12] In this report we characterize the rate of accumulation of lipofuscin at different sites in the posterior pole and compare these rates with previously reported data from ex vivo[1,38,39] and in vivo[12,37,40] studies. If lipofuscin is a marker for areas of the fundus at great risk for pathology, it would be important to know what mechanisms produce its distribution. Lipofuscin distribution along the horizontal meridian has only been characterized with low spatial resolution, but the distribution along the vertical meridian is not known. We also investigate how lipofuscin is spatially distributed across the

From the [1]Schepens Eye Research Institute and [2]Harvard Medical School, Boston; and [3]R&D Consulting, Arlington, Massachusetts.

Supported by National Institutes of Health Grant EY8511 and grants from the Massachusetts Lions Eye Research Fund, Inc., and the Retina Research Foundation, Houston, Texas.

Submitted for publication December 1, 2000; revised February 21, 2001; accepted March 9, 2001.

Commercial relationships policy: N.

The publication costs of this article were defrayed in part by page charge payment. This article must therefore be marked "*advertisement*" in accordance with 18 U.S.C. §1734 solely to indicate this fact.

Corresponding author: François C. Delori, Schepens Eye Research Institute, 20 Staniford Street, Boston, MA 02114.
delori@vision.eri.harvard.edu

Table 1. Population

	n	F/M	Age (years)*	Age Distribution (Subjects/Decade) 2	3	4	5	6	7	8
All subjects (at *F* and 7° T)	145	71/74	50 ± 18	4	23	20	22	26	27	23
Subgroups										
A: At 7° T, N, S, I	37	16/21	53 ± 15	0	5	4	5	7	16	10†
B: Imaging (central; 0–4.5°)	16	7/9	58 ± 9	0	0	0	3	6	7	0
C: Along meridians (7–30°)	7	2/5	51 ± 12	0	0	3	1	3	0	0

n, number of subjects. Measurement sites: F, fovea; T, temporal to the fovea; N, S, and I: nasal, superior, and inferior to the fovea, respectively.
* Values are mean ± SD.
† Measurement in these 10 subjects were not included in subgroup A and were used only to document the decline in fluorescence at old ages.

fundus, tested whether there are age-related changes in distribution, and compared the distribution of lipofuscin with published distributions of photoreceptors,[41,42] macular pigment,[43] and lesions in ARM.[44] The ultimate goal of our research is to evaluate whether peak levels of lipofuscin identify eyes at high risk for subsequent photoreceptor loss and to determine whether focal decreases in lipofuscin content identify regions where photoreceptor loss is occurring.

Methods

Subjects

The study population consisted of 145 subjects (age range, 15–80 years) with normal retinal status and no systemic disease other than hypertension. Age and gender distribution for all experimental subgroups are detailed in Table 1. All subjects were whites of European descent, had best corrected visual acuity of 0.63 or better, refraction between −6 and +4 diopters, and no ocular pathology. Classifying the iris color as light (blue, green, or gray iris) or dark (hazel or brown iris) characterized ocular pigmentation. Twenty-two older subjects had few hard drusen (<10 in a 10° diameter circle centered on the fovea); these are considered to be nonpathologic aging changes.[45] Subjects with mild and moderate nuclear sclerosis were included if their crystalline lens optical density at 510 nm was lower than 0.375 DU (density units), to minimize errors in the correction for lens absorption (explained later).[46] Spectrophotometric measurements of autofluorescence were performed at the fovea and at 7° temporal to the fovea in all subjects; in 37 subjects additional measurements were made at 7° nasal, inferior, and superior to the fovea (subgroup A, Table 1). High-resolution autofluorescence images of the foveal area (up to 4.5° eccentricity) were recorded in 16 subjects (subgroup B) to measure the central spatial distribution. Finally, spectrophotometric measurements were made along the four cardinal meridians between 7 and 30° from the fovea in seven subjects (subgroup C).

The tenets of the Declaration of Helsinki were followed, Institutional Review Board approval was granted, and informed consent was obtained for all subjects. The pupil of the test eye was dilated with 1% Tropicamide to at least 7 mm in diameter. All light levels used in the noninvasive measurement of lipofuscin were within the safety limits recommended by the ANSI standards.[34]

Spectrophotometry

Data were acquired by fundus spectrophotometry[34] according to established protocols.[47] The subject's pupil was aligned under infrared illumination, and the fundus was observed with 540 to 620-nm light. Excitation light, derived from a Xenon arc lamp with an excitation filter centered at 550 nm (FWHM, 20 nm), irradiated a 3° diameter retinal field during 180 ms (radiant exposures, 10–17 mJ/cm^2). The fluorescence was collected from a sampling field (centered in the excitation field) with a diameter of 2° (585 μm). After rejection of reflected excitation light by a barrier filter, the fluorescence was spectrally analyzed by an optical multichannel analyzer (Princeton Applied Research, Trenton, NJ) producing an emission spectrum with a spectral resolution of 6 nm. The contribution of lens fluorescence and scatter was measured[34] in each subject and subtracted from the fundus fluorescence spectrum (this correction was <5% for the population studied here).

An internal fixation was used to direct the subject's fixation for sites within 7° from the fovea. External fixations were used for measurements at larger eccentricities, 10 to 30°, and test sites were marked on a fundus photograph. Each measurement was preceded by a 510-nm bleaching exposure of 7.1 log photopic trolands for 2 seconds, sufficient to bleach 99.8% of the cones and >85% of the rods;[48]; the error in the fluorescence measurement resulting from this incomplete rhodopsin bleach is ≈3% (compared with ≈20% if we did not bleach). As much as possible, large vessels were avoided by slight displacements, and focus and pupil position were readjusted before each measurement.

Fluorescence Imaging

Images of fundus autofluorescence centered on the fovea were obtained with a modified fundus camera (TRC-FE; Topcon Corp., Tokyo, Japan) coupled to a CCD camera.[36] The retinal field was restricted to a 13°-diameter circle to minimize contributions of light scattering and fluorescence from the crystalline lens. Alignment and focusing was performed under 550-nm illumination. Fluorescence images were obtained with flash settings of 300 W·sec using 470- and 550-nm excitation filters (FWHM ≈30 nm) and matched barrier filters. Retinal exposure for autofluorescence imaging was 3 to 5 mJ/cm^2 (duration, 1–2 msec). Retinal images were recorded with a cooled scientific grade CCD camera (768 × 512 pixels, MicroMax; Princeton Instruments, Trenton, NJ). Areas of 2 × 2 pixels were combined to 1 pixel; the size of this pixel was 15.6 μm at the retina. Gray levels for fundus fluorescence were typically 50 to 200.

Correction for Lens Absorption

Because the fluorescence excitation and emission are affected by crystalline lens absorption, and because the latter is strongly affected by age,[49,50] it is necessary to individually correct the fluorescence data to account for the loss of light in the lens. This is achieved by using a previously described reflectometry method.[46] In essence, a reflectance spectrum was recorded at 7° temporal to the fovea using the same optical path in the eye as for the fluorescence measurements. The difference in the log-reflectances at 520 and 485 nm is equal to the difference of 2 terms: (1) the difference in log-reflectances at the same wavelengths in absence of ocular media, and (2) two times the lens optical density difference between 485 and 520 nm (double pass). Assuming that the first term is unaffected by age (or that its age variation is small compared with that of the second term) and using known extinction coefficients for the lens,[49] one can derive the lens optical density at 510 nm relative to the mean lens density at an age of 44 years. The relative lens optical densities estimated by this method

vary between −0.15 to 0.4 DU at 510 nm, are reproducible within 0.05 DU, are not affected by ocular pigmentation, and are not statistically different from lens optical densities determined psychophysically in the same subjects.[46]

Data Analysis

All fluorescence spectra were individually corrected for the excitation energies, for the spectral sensitivity of the detecting system,[34] and for the absorption by the crystalline lens (see above). Emission spectra, obtained with an excitation at 550 nm, were integrated between 650 and 750 nm to yield the fluorescence measure (fluorescence units [FU] are in $\mu J \cdot sr^{-1}/J$). Although the emission spectrum extends from 550 to 800 nm with a maximum at ≈640 nm (Exc, 550 nm),[37] we used only the emission above 650 nm, to minimize contributions from secondary fluorophores.[51] The excitation at 550 nm (FWHM, 20 nm) is minimally affected by macular pigment absorption: optical density of the macular pigment is generally <1 DU at 460 nm and therefore < 0.015 DU (3% absorption) at 550 nm.[52] Absorption by RPE melanin should also be minimized by the choice of excitation and detection wavelengths because the absorption by melanin decreases monotonically throughout the visible spectrum.[53]

Autofluorescence images at 470- and 550-nm excitation were analyzed using the IGOR image analysis software (WaveMetrics, Lake Oswego, OR). The 550- and 470-nm images were aligned using translations and matching the position of retinal landmarks in the superimposed images. The position of the center of the fovea was defined as the location with lowest fluorescence in the 470-nm image; this corresponds with the location of the highest macular pigment density (highest concentration of cones). Horizontal and vertical profiles through the center of the fovea, averaged over 5 pixels (77 μm), were calculated for the 550-nm images and normalized to the average level in a 2° diameter circle centered on the fovea. Maximal eccentricity was 4.5°, avoiding areas of nonuniformity of excitation at the edges of the 13° diameter image.

Results

Lens Optical Density

The optical density of the crystalline lens for the subjects of this study (Fig. 1) was significantly and positively correlated with age ($r = 0.92$; $P < 0.0001$). The density exhibited an accelerating increase with age that can be described by a fourth degree polynomial (curve A in Fig. 1). A slight decrease in acceleration was evident for ages > 65 years. The density at 510 nm increased from an average (±SD) of −0.07 ± 0.01 DU at age 25 to an average of 0.15 ± 0.07 DU at age 65 (referenced to the mean optical density at 44 years). Application of this correction to the fluorescence data (Exc, 550 nm; Em, 650 nm) resulted in a mean increase of the fluorescence by a factor ≈1.25 at age 65 and a factor ≈0.89 at age 25.

Lipofuscin Accumulation

After correction for lens absorption, the spectra of fundus autofluorescence excited at 550 nm had a mean maximum (±SD) at 640 ± 11 nm ($n = 145$), and the spectra dropped to half their peak intensity at 725 to 750 nm. Maximum emission shifted toward shorter wavelengths with excitation at shorter wavelengths: the mean peak wavelength for 430-nm excitation was 608 ± 14 nm. The integrated fluorescence (650–750 nm) for 550-nm excitation (used in this study) correlated highly with measurements of peak fluorescence obtained with excitations between 420 and 560 nm ($r > 0.88$; $P < 0.0001$). This confirms that one dominant fluorophore is sampled in vivo; its spectral characteristics have been shown to be consistent with lipofuscin.[37]

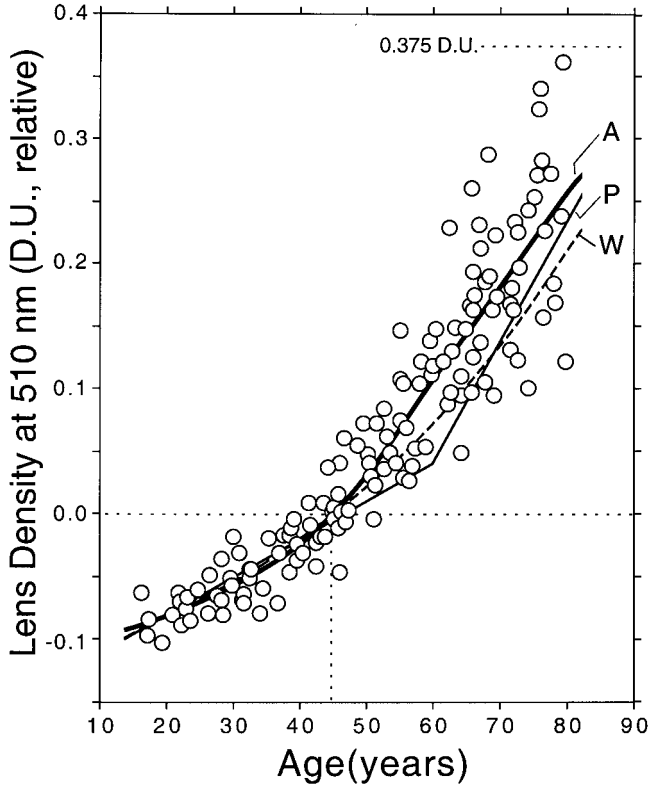

Figure 1. Crystalline lens optical density at 510 nm as a function of age. This density is the difference between the lens density of an individual and the mean lens density at age 44. The *solid curve* (**A**) is a fourth degree polynomial fitted to the data: $5.9 \times 10^{-2} \cdot \alpha + 1.17 \times 10^{-4} \cdot \alpha^2 - 6.08 \times 10^{-7} \cdot \alpha^3 - 4.09 \times 10^{-8} \cdot \alpha^4$ ($r^2 = 0.87$), where α = (age 44). The average lens optical density at 510 nm predicted for each age by the algorithm of Pokorny et al.[49] (*thin solid lines,* P) and of Weale[50] (*interrupted line*, W) and normalized at age 44 is shown for comparison. Subjects with lens density > 0.375 DU were excluded from the study.

Lipofuscin fluorescence, corrected for lens absorption (Fig. 2), exhibited a significant positive correlation with age ($r = 0.73$ and $r = 0.69$ for the temporal site and the fovea, respectively; $P < 0.0001$). The fluorescence in the fovea was significantly less than that at 7° temporal to the fovea ($P < 0.0001$, paired *t*-test, two-tailed), being on average 61% ± 9% of the value at 7° temporal. The fluorescence increased quasi-linearly up to approximately 70 years of age and then decreased in older subjects.

The variation in lipofuscin content in subjects between ages 20 and 70 years ($n = 118$) was best described by a linear regression; quadratic regressions did not yield a significant second-degree terms ($P > 0.3$). Regression equations $F(\text{age}) = F(25) + \text{ARA} \cdot (\text{Age} - 25)$ fitted to the fluorescence yielded values for $F(25)$, the mean fluorescence at age 25 (intercept), and ARA, the absolute rate of accumulation (slope), given in Table 2. The values for $F(25)$ at the 7° temporal site and at the fovea were, respectively, 8.8 and 5.6 FU, and the ARAs were 0.39 and 0.24 FU/y. Both $F(25)$ and ARA were significantly lower at the fovea than at 7° temporal to the fovea. The fluorescence at age 65 was ≈2.8 times greater than that at age 25 for both sites; this ratio would be ≈2.0 for fluorescences not corrected for lens absorption (see above).

For the 37 subjects in subgroup A (age range, 20–70 years) with measurements at 7° eccentricity along all four meridians (Table 1), we found that the accumulation rates (ARA) at the temporal, nasal, superior, and inferior sites were 0.35 ± 0.05,

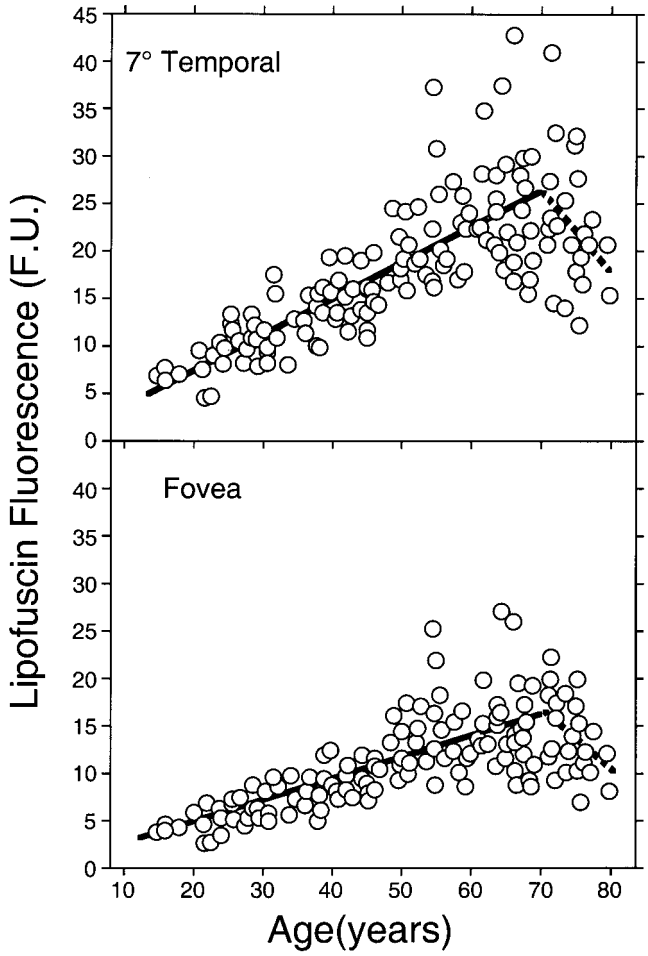

Figure 2. Lipofuscin fluorescence as a function of age at 7° temporal to the fovea (*top*) and at the fovea (*bottom*). The *solid lines* are linear regression lines for ages 20 to 70 years ($P < 0.0001$). The *interrupted lines* are linear regression lines for ages 70 to 80 years ($P < 0.12$). Results of regression analysis are in Table 2.

0.29 ± 0.04, 0.31 ± 0.04 and 0.24 ± 0.04 FU/y (±SE), respectively, and the estimated $F(25)$ were 9.5 ± 1.5, 10.2 ± 1.3, 8.6 ± 1.3, and 9.2 ± 1.3 FU ($r^2 = 0.60$, 0.57, 0.61, and 0.50, respectively). Analysis of variance demonstrated that the ARAs and $F(25)$s at these four sites were not significantly different from each other ($P > 0.2$), except for a tendency for the ARA to be smaller inferiorly than superiorly ($P = 0.08$).

The fluorescence exhibited a tendency to decline above age ≈70 years (Fig. 2); the rate of decline was estimated by regression analysis for the 23 subjects over age 70. The slopes of the regression lines for the temporal site and the fovea were −0.86 and −0.63 FU/y, respectively (Table 2), not significantly different from each other. Both slopes were significantly smaller than the rate of accumulation for ages < 70 years ($P < 0.0001$). Similar decreases in the accumulation rate were found at 7° eccentricity along the superior, inferior, and nasal meridians in 10 subjects over age 70 (Table 1). The slopes were about −1.5 FU/y and were also significantly smaller than the accumulation rates for ages < 70 years of age ($P < 0.01$).

The fluorescence measurements at the five sites (fovea and 7° from the fovea on each meridian) were highly correlated with each other ($r > 0.88$, $n = 37$, $P < 0.0001$, for all possible combinations). After accounting for the age dependence at each site, the "remaining variation in fluorescence" was still highly correlated between the five sites ($r > 0.83$, $P < 0.0001$). This means that if the fluorescence was high or low at one site for a given age, it was also high or low at the other sites. The same intraindividual correspondence was seen in the high interocular correlation in fluorescence found in 10 subjects ($P < 0.0005$ for both sites); there was no significant difference between the estimates in both eyes (paired, both $P > 0.2$).

Spatial Distribution

Spatial distributions were measured in three subgroups of subjects (Table 1) using spectrophotometry in four sites at 7° from the fovea on the four meridians (subgroup A), using fluorescence imaging in a central 9° diameter circle (subgroup B) and using spectrophotometry along the four meridians at eccentricities between 7 and 30° (subgroup C). Measurements in each subgroup included a measurement at the fovea. Fluorescence at each eccentricity was expressed as $\Phi(r)$, the ratio of the fluorescence at eccentricity r (in degrees) and that at the fovea. Positive eccentricities are for the temporal and superior directions and negative for the nasal and inferior directions.

Subgroup A. The spectrophotometric ratios $\Phi(\pm 7°)$ in the four cardinal directions in 37 subjects were all significantly different from each other (Table 3; subgroup A). The fluorescence was highest temporally, then nasally, superiorly, and lowest inferiorly. Values at eccentricity were all significantly larger than at the fovea ($P < 0.001$). The ratios $\Phi(\pm 7°)$ were

Table 2. Linear Regression of Fluorescence of Lipofuscin Versus Age

	Site of Measurement		
	7° Temporal*	Fovea*	*P*†
Age range, 20–70 years; $n = 118$; $F(\text{age}) = F(25) + \text{ARA} * (\text{age} - 25)$			
Fluorescence $F(25)$ (FU)	8.8 ± 0.7	5.6 ± 0.5	0.0002
Rate ARA (FU/y)	0.39 ± 0.03	0.24 ± 0.02	<0.0001
Fluorescence $F(65)$ (FU)	24.6 ± 0.7	15.1 ± 0.5	<0.0001
r^2, P	0.63, $P < 0.0001$	0.56, $P < 0.0001$	—
Ratio $F(65)/F(25)$	2.83 ± 0.08	2.80 ± 0.09	0.85
Age range, 70–80 years; $n = 23$; $F(\text{age}) = F(70) + \text{ARA} * (\text{age} - 70)$			
Fluorescence $F(70)$ (FU)	26.5 ± 2.8	16.7 ± 1.6	0.004
Rate ARA (FU/y)	−0.86 ± 0.52	−0.63 ± 0.29	0.70
r^2, P	0.11, $P = 0.12$	0.18, $P = 0.04$	—

ARA, absolute accumulation rate; FU, fluorescence unit.

* Values are means ± SE.

† Statistical significance of the difference between 7° temporal and the fovea.

TABLE 3. Fluorescence Along Meridians Relative to That at the Fovea (Age Range, 20–70 Years)

Φ(r)*	Subgroup/*n**	Temporal	Nasal	Superior	Inferior
Φ(±2)	B/16	1.18 ± 0.07 NsI	1.08 ± 0.11 T	1.12 ± 0.09 t	1.10 ± 0.11 T
Φ(±4)	B/16	1.35 ± 0.08 sI	1.33 ± 0.13 I	1.28 ± 0.12 ti	1.20 ± 0.12 TNs
Φ(±7)†	A/37	1.66 ± 0.23 nSI	1.59 ± 0.26 tSI	1.48 ± 0.25 TNI	1.38 ± 0.21 TNS
$\Phi(r_{max})$ at r_{max}‡	C/7	1.69 ± 0.17 11.2 ± 2.2°	1.67 ± 0.21 −6.9 ± 0.4°	1.71 ± 0.29 12.7 ± 3.4°	1.41 ± 0.12 −8.6 ± 2.0°
Φ(±21)	C/7	1.36 ± 0.24 ni	1.49 ± 0.26 tI	1.51 ± 0.29 i	1.19 ± 0.18 tNs
Φ(±27)	C/6	1.04 ± 0.17 —	1.17 ± 0.33 —	1.25 ± 0.17 —	0.97 ± 0.22 —

Values are mean ± SE.

* $\Phi(r)$ is the fluorescence at eccentricity r relative to that at the fovea ($r=0$, $\Phi(0)=1$). Subgroup A, B and C refer to subgroups defined in Table 1. Statistically significant difference between sites (two-tailed paired *t*-tests) is indicated by the letters "TNSI" ($P < 0.005$) or "tnsi" ($0.005 < P < 0.05$). Thus, the fluorescence at 2° nasal (T) was significantly different from that at 2° temporal, but not statistically different from that at the two other sites.

† Fluorescence ratios Φ(±7) measured in subgroup C (not shown) were not significantly different than those measured in subgroup A at ± 7°.

‡ r_{max} is the eccentricity at which the fluorescence, $\Phi(r_{max})$, is maximal along each meridian.

not significantly influenced by ocular pigmentation (as judged by iris color, $P > 0.5$). Comparing only the sites at 7° eccentricity, one finds no correlation with age for the ratios of nasal to temporal ($\rho = -0.19$; $P = 0.2$) and superior to temporal ($\rho = -0.0$; $P = 0.9$) fluorescence, but a significant negative correlation ratio of inferior to superior fluorescence ($\rho = -0.43$; $P = 0.009$). Linear regression of the difference between the inferior and superior fluorescences with age suggests that the fluorescences are about equal at age 25 (difference = 0.5 ± 0.7 FU; $P = 0.4$) but that it then increases less rapidly in the inferior than in the superior fundus ($P = 0.005$).

Subgroup B. The individual distributions obtained from imaging ($n = 16$) along the horizontal and vertical meridians (Fig. 3) demonstrate large variations in the shape of the foveal depression ranging from very shallow to deep (Φ (±4) = 1.07 − 1.58). Average results for Φ (2°) and Φ (4°) are given in Table 3 (subgroup B). The relative distribution of fluorescence along the meridians follow a pattern similar to that seen at 7° from the fovea (subgroup A): fluorescence is highest temporally and lowest inferiorly. Statistical differences in Φ at the same eccentricity were most pronounced between the temporal and inferior meridians, and least so between the nasal and superior meridians. None of the Φ (*r*) ratios correlated significantly with age and degree of ocular pigmentation.

The position of minimal fluorescence was calculated using a 0.5° moving average of the profiles in Figure 3. The minima along the horizontal and vertical meridians were on average at −0.40 ± 0.60° and −0.35 ± 0.57° from the fovea, respectively, and both were significantly different from 0 ($P = 0.02$ and $P = 0.03$, respectively). Because the position of these minima were highly correlated with each other ($r = 0.61$; $P = 0.009$), it suggests that the location of the minimum fluorescence is slightly displaced toward the nasal-inferior side of the fovea. Isofluorescence contours for fluorescence 10% higher than that at the fovea exhibited a circular shape; the horizontal and vertical widths were 2.77 ± 0.83° and 2.81 ± 0.79°, respectively (paired test, $P = 0.8$). However, the contour for fluorescence 15% higher than at the fovea was found to be elliptical with a longer vertical axis. The horizontal and vertical widths were 3.3 ± 1.2° and 4.3 ± 1.0°, respectively ($P = 0.02$; $n = 15$).

Subgroup C. The individual distributions of fluorescence along the horizontal–vertical meridians derived from spectrophotometry ($n = 7$; Fig. 4) and the average results in Table 3 (subgroup C) exhibit the same asymmetries observed at lower eccentricities: fluorescence was highest temporally and superiorly, and lowest inferiorly. The fluorescence decreased in the peripapillary region and was further reduced over the optic disc itself (Φ = 0.1 to 0.8 in the disc, with a different spectrum

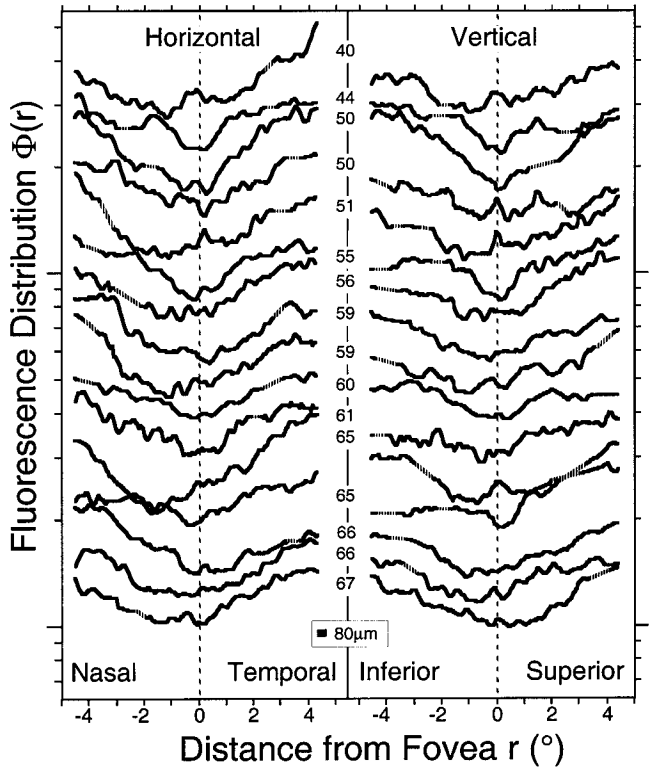

FIGURE 3. Autofluorescence distribution measured by imaging in 16 subjects (subgroup B, ages indicated in the *middle*) along the horizontal (*left*) and vertical meridian (*right*) through the fovea. The spatial resolution is 0.27° or 80 μm (*box*). The fluorescence are expressed by Φ (*r*), the ratio of the fluorescence at an eccentricity *r* to that at the fovea. Individual pairs of traces were displaced vertically along the logarithmic scale to avoid overlap. *Dashed portions of the curves,* areas that were interpolated to remove the attenuation due to vessels as seen on the autofluorescence image.

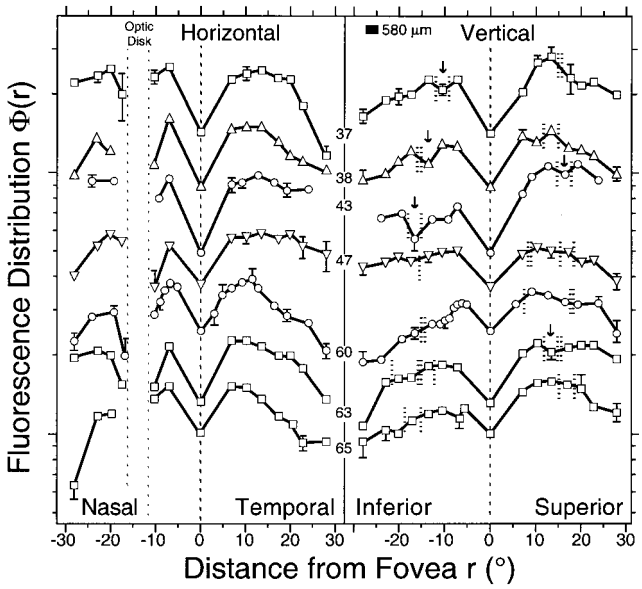

FIGURE 4. Spatial distribution of autofluorescence along the horizontal (*left*) and vertical (*right*) meridian through the fovea for seven subjects (ages shown in center, subgroup C). The spatial resolution is 2° or 580 μm (*top middle*). Φ (*r*) is the fluorescence at eccentricity *r* relative to that at the fovea. The traces were displaced vertically in both panels to avoid overlap. Each *point* represents the average of two or three measurements done without repositioning and the error bars are ± SD (error bars less than ±0.05 were removed). *Vertical interrupted bars,* the approximate position of vessels (50–100 μm diameter) crossing the meridians. It is likely that retinal vessels compounded by eye movements caused some of the "dips" observed on the vertical profiles. Indeed, there was a 1- to 2-second delay between the aiming and the actual measurement, and there was often little space for our sampling field between the vessels. When we purposely included a vessel in our sampling field, we observed a decrease similar to that observed in some profiles. *Vertical downward arrows,* those instances in which we interpolated the data between neighboring points, to obtain the average data presented in Table 3 and Figure 5.

as previously shown.[34] The fluorescence at all sites for eccentricities up to ≈20° (and outside the disc area) were significantly higher than that at the fovea. The ratios Φ (*r*) were not significantly correlated with age, except for Φ (−7) on the inferior meridian that was negatively correlated with age ($\rho = -0.86$, $P = 0.03$).

Peak fluorescence along the meridians occurred at 9 to 14° from the fovea temporally (averages in Table 3), at 10 to 19° superiorly, and at −6 to −11° inferiorly. Maximal fluorescence on the nasal side of the fovea generally occurred between the disc and the fovea at ≈ −7°; a second maximum was observed nasal to the disc at −19 to −23° from the fovea (mean, −21 ± 2°; Φ = 1.52 ± 0.28). The highest maximum Φ (r_{max}) occurred along the superior and temporal meridians, whereas the lowest occurred along the inferior meridian (Table 3).

Figure 5 summarizes the average results obtained in the three different series of measurements. Starting from the central minimum, fluorescence rises more steeply in the temporal and nasal directions than in the superior and inferior directions. A discontinuity in distribution occurs between the horizontal and vertical profiles at ≈ 2° from the fovea. The fluorescence is maximal in a ring located at an eccentricity of 9 to 13°. The fluorescence along the inferior meridian is always less than along the other meridians at the same eccentricity. By 20° eccentricity, the fluorescence is found to be highest along the superior and nasal meridians, followed by that along the temporal and inferior meridians.

DISCUSSION

We have shown that lipofuscin accumulates quasi-linearly in the RPE between the ages of 20 and 70 years and that it decreases in the 8th decade of life. The rate of accumulation was approximately 0.4 FU/y at an eccentricity of 7° and was significantly lower in the fovea. Fluorescences at different sites were significantly correlated with each other, indicating that if the fluorescence in an individual is high or low at one site, it is also high or low at other sites at the posterior pole of the eye. These observations, as well as the high interocular correlation, suggest that the distribution is determined by some intrinsic characteristic of the eye (e.g., density of photoreceptors, number of photoreceptors/RPE cells, distribution of vitamin A transporters), whereas the quantity of lipofuscin accumulated at all sites reflects individual variables (e.g., antioxidant status, diet, genetics, ocular pigmentation, exposure to xenobiotic agents, and/or possibly light exposure).

Age-Related Accumulation of Lipofuscin

We found a significant age-related accumulation of lipofuscin (Fig. 2, Table 2), confirming previous ex vivo[1,38,39] and in vivo[12,37,40] reports that lipofuscin increases with age (Fig. 6). Our results affirm the monotonic rate of increase observed in our earlier studies[12,37] and in those of von Rückman et al.[40] In contrast, earlier ex vivo observations suggested that deposition of lipofuscin varied with age. To compare the rates of age-related increase in fluorescence and lipofuscin, we used the ratio of fluorescence at age 65 to that at age 25 (Fig. 6, inset), which was ≈2.8 in this study (Table 2).

Comparison with Other In Vivo and Ex Vivo Studies

Von Rückmann and colleagues[40] used the Laser Scanning Ophthalmoscope to measure fluorescence at 7 to 15° temporal to the fovea in normal subjects. Their data, corrected to account for average lens absorption at a given age either using Pokorny[49] algorithm (curve V; Fig. 6) or using the mean of our lens correction (curve V′), show a faster accumulation than that found in this study (curve D). Possible explanations for this faster accumulation include differences in excitation wavelength and in subject selection. We measured the fluorescence excited at 550 nm (Em > 650 nm); von Rückmann used a 488-nm excitation (Em > 520 nm). Indeed, we found a faster age-related increase in our data obtained with 470-nm excitation (acquired in our standard protocol) and integrating all fluorescence >520 nm (curve D′, Fig. 6). The fact that von Rückmann included only patients "with clear lenses," whereas ours included subjects with mild to moderate nuclear sclerosis, may explain why the application of our correction (V′) resulted in an overestimation of lipofuscin content at older ages.

Ex vivo measurements of fluorescence[38,39] or counts of lipofuscin granules[1] in sectioned donor eyes (curves W, O, and F in Fig. 6) all indicated significant increases with age, but the rates of accumulation were substantially lower. Several factors (reviewed by Okubo[39]) may have contributed to an underestimate of lipofuscin accumulation in the ex vivo studies. The age-related change in fluorophore composition of the granules[54] may cause an age-related increase in the fraction of fluorophores extracted by organic solvents during the embedding process. Rates determined by fluorescence were slightly higher than those determined by granule counts, possibly because fluorescence of lipofuscin granules increases with age.[54]

Lipofuscin and melanin granules have overlapping distributions within the RPE cell. The concentration of melanin in the apical cytoplasm exceeds that in the basal cytoplasm by a factor of ~1.5, whereas basal lipofuscin concentration exceeds

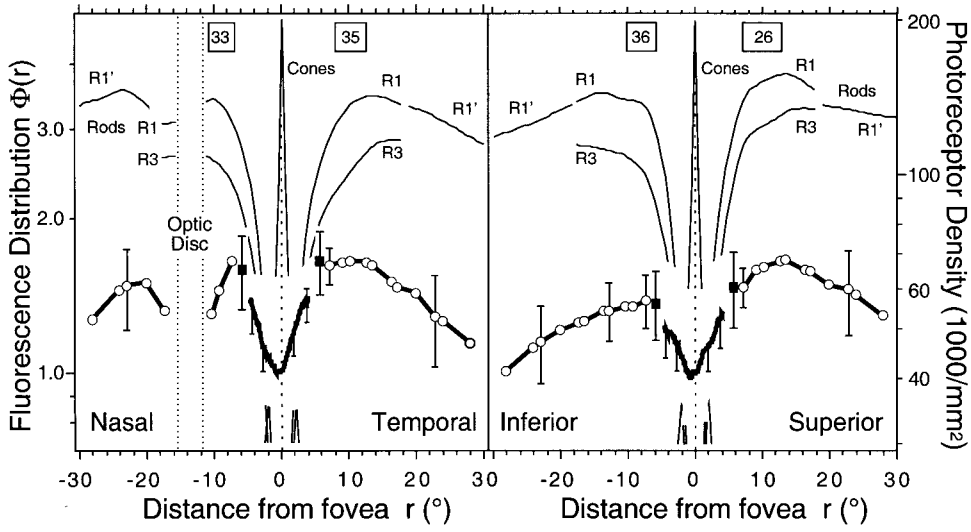

FIGURE 5. Average spatial distribution of autofluorescence along the horizontal (*left*) and vertical (*right*) meridians (*thick line*; *left scale*). The data were obtained from imaging (*V-shaped curves* at *center*) in 16 subjects (Fig. 3), from spectrophotometric estimates (*solid square symbols*) of Φ (7) along the four cardinal meridians in 37 subjects (Table 3) and from spectrophotometric measurements (*open circles*) of Φ (*r*) at eccentricities of $r = 7$ to 30° from the fovea in 7 subjects (Fig. 4). All data were normalized at the fovea ($\Phi(0) = 1$). Error bars are representative intersubject SD. The distributions of cone and rod density, determined by Curcio and colleagues,[41,42] are shown as *thin lines* (*right scale*). Rod distributions are R1 and R3 for 27 to 37 and 61 to 75 years donor eyes, respectively (Curcio's groups 1 and 3).[42] At larger eccentricities, curve R1′ is for 27 to 44 years donor eyes.[41] The *bars* at the *top* of each panel indicate those regions where rod loss between groups 1 and 3 are highest;[42] the peak loss in rods/mm^2 × 1000 is indicated in each *bar* and the *bar widths* represent losses > 90% of peak loss. Photoreceptors and fluorescence distribution can be compared because both *left* and *right* full scales represent a 6.6-fold range (logarithmic scales). Numerical data for the distribution of rods along the meridians (Fig. 6 in Curcio et al.[42]) were provided by Christine Curcio (University of Alabama, Birmingham, AL).

apical concentration by ~1.4.[2] Microscopic measurements are made with a fixed sampling area in central regions of the cell that are relatively free of melanin, whereas both the excitation and emission light for in vivo measurements will be partially absorbed by the apical layer of RPE melanin. Whether this attenuation is affected by age depends on both changes in absorption by melanin and changes in the relative distribution of both pigments. The number of RPE melanin granules decreases with age,[1] but the size and optical density of the granules increase.[54] These opposing effects may explain why no age-related changes were found in macular RPE melanin concentration,[55] optical density of the RPE (except perhaps above age 50),[2] or in reflectometric estimates of the melanin optical density difference between the fovea and the perifovea.[51] However, even if the total optical density does not significantly change with age, melanin distribution is affected by age. Melanin in the first decade of life is entirely apical, but with increasing age the distribution becomes more uniform (by age 70, at least half of the melanin granules are embedded in complex melanolipofuscin granules).[2,56] Thus, in vivo measurements of lipofuscin in younger eyes are more underestimated because of screening by apical melanin, and this would result in an exaggerated estimate of the age-related increase in lipofuscin fluorescence measured in vivo.

If we assume that the difference between the accumulation rates estimated from the in vivo data (curve D, Fig. 6) and from the ex vivo data (average of curves O and W) is entirely due to melanin, we can estimate that melanin must have attenuated lipofuscin fluorescence 1.5 times more at age 15 than at age 65. We can calculate F_{15}, the fluorescence in young subjects, with all the melanin located apical to the lipofuscin and F_{65}, the fluorescence in old subjects, with the melanin uniformly intermixed with lipofuscin in the entire cell. These fluorescences are given by:

$$F_{15} = \zeta \cdot d \cdot 10^{-[K_\Lambda + K_\lambda] \cdot D_{500}}$$

and

$$F_{65} = \frac{\zeta \cdot d \cdot \{1 - 10^{-[K_\Lambda + K_\lambda] \cdot D_{500}}\}}{\ln(10) \cdot [K_\Lambda + K_\lambda] \cdot D_{500}}$$

where ζ is the efficiency of the lipofuscin fluorescence (per unit length), d the total thickness of the RPE, K_Λ and K_λ the extinction coefficients of melanin[53] at the excitation (Λ) and emission (λ) wavelength (normalized to the extinction at 500 nm), and D_{500} is the melanin optical density of the RPE at 500 nm. The latter is the same in both cases; we assume a very thin apical layer with high concentration at age 15, and the full thickness d with low concentration at age 65. Substituting $F_{65} = 1.5$. F_{15} ($\Lambda = 550$ nm, $\lambda = 650$ nm), we found by successive approximation a value $D_{500} = 0.32$ DU. For the data with $\Lambda = 470$ nm (curve D′), we similarly found an optical density of $D_{500} = 0.29$ DU. These results are consistent with the mean optical densities for the entire RPE of 0.23 DU[2] and 0.35 DU[53] measured ex vivo at 500 nm. Although derived from different studies, these calculations indicate that most of the difference in accumulation rates between ex vivo and in vivo estimates could be accounted for by a redistribution of melanin within the RPE cell, even though the total amount of melanin remains constant.

Decline in Lipofuscin Fluorescence at Older Ages

The lipofuscin levels observed above age 70 were lower than would be expected if lipofuscin accumulated at a constant rate throughout life (Fig. 2). Other studies (Fig. 6) have not detected significant evidence that lipofuscin levels decline above age 70, although only a few demonstrate significant increases at old age. The gradual age-related loss of rod photoreceptors throughout life[42,57] cannot explain the sudden decrease in lipofuscin above age 70. We cannot exclude the possibility that individuals with higher lipofuscin content have developed AMD and are thus excluded from this study or that individuals with the highest lipofuscin are selectively eliminated from the study because they are less healthy at advanced age and/or may have higher mortality rates. It is worth noting that some of the 50- to 70-year-old subjects have very high lipofuscin (Fig. 2).

The decrease in fluorescence at ages > 70 could also result, in part, from an undercorrection by our lens optical density estimates.[46] Although our average lens densities are slightly higher than those predicted in other studies[49,50] at old age (Fig. 1), they exhibit a slight reduction in acceleration at older age. We believe that this may indicate some underestimation of the

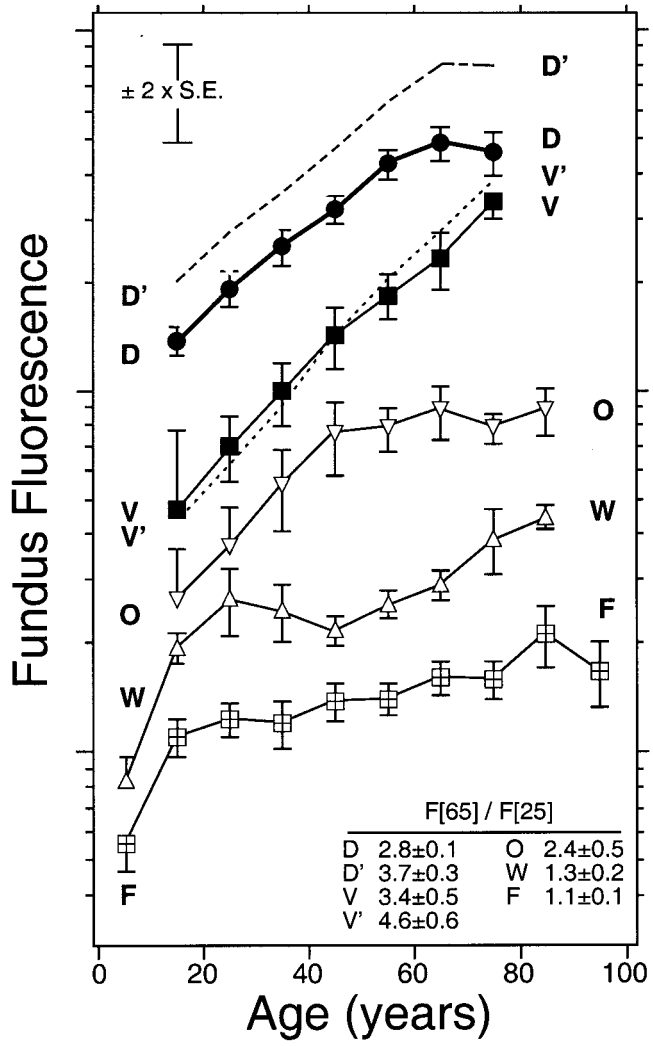

FIGURE 6. Age relationship of autofluorescence for this study (D) and other studies from the literature. Fluorescence, averaged in each decade, is plotted on a logarithmic scale and was displaced vertically for clarity. *Closed* and *open symbols:* for in vivo and ex vivo measurements, respectively. D and D′: obtained in this study with excitations at 550 nm (Fig. 2, temporal site) and 470 nm, respectively (20–27 subjects/decade). V and V′: measured by Von Rückmann et al.[40] using the Laser Scanning Ophthalmoscope (Exc, 488 nm, 5 subjects/decade) with correction to account for lens absorption using the algorithm of Pokorny et al. (Fig. 1; curve P),[49] and the mean lens optical density derived in our population (Fig. 1, curve A). O and W: measured ex vivo using fluorescence microscopy on section of RPE; curve O is from Okubo et al.[39] (Exc, 450–490 nm, 5–14 eyes/decade), and curve W from Wing et al.[38] (Exc, 390–470 nm, 2–8 eyes/decade).[38] Finally, curve F is from the combined counts of lipofuscin and melanolipofuscin granules performed by Feeney et al.[1] (1–5 eyes/decade). The *inserted table* gives the values of $F(65)/F(25)$ for each of set of data.

lens optical density and is the reason why we excluded subjects with lens densities > 0.375 DU. To support a linear age-related accumulation of fluorescence up to age 80 (Fig. 2), the extrapolated fluorescence at age 80 would need to be 1.7 times greater than that measured, on average, at age 80. This would require an incremental density of 0.3 DU (510 nm) between the ages of 65 and 80 and would double the lens density at age 80. Because this is clearly unreasonable, we can reject gross underestimation of lens absorption as the sole reason for the decline in fluorescence. Some undercorrection may exist, but we are not able to assess its magnitude; future studies comparing fluorescence before and after IOL surgery may clarify this issue.

Previous reports have shown that lipofuscin levels in those with AMD were significantly below normal subjects of the same age[6,33] and that fluorescence in regions of geographic atrophy is very low.[7,37,40,58] Current evidence, reviewed in the Introduction, indicates that A2E (a major constituent of lipofuscin) will cause RPE apoptosis if it is released from the lysosomes into the cytoplasm[31] or if it mediates blue-light damage.[27] Subsequent removal of apoptotic RPE cells would result in local reduction in lipofuscin fluorescence. The possibility that the decrease in RPE lipofuscin in older subjects represents incipient atrophy may be supported by our observation in autofluorescence imaging of substantial focal variability in fluorescence and small patches of very low fluorescence in 3 of 10 subjects (60–70 years old). A more rigorous quantitative analysis is required to elucidate whether the regions of low fluorescence represent regions of reduced photoreceptor density and/or incipient atrophy.

The magnitude of the contribution of A2E to in vivo fluorescence measurements is still unknown. Emission spectra of A2E (Exc, 380 nm) in different organic and inorganic solvents have a maximum at 570 to 610 nm, and intracellular A2E has a maximum emission at 560 to 575 nm.[30] Excitation and absorption maxima of A2E in the visible range occur at 430 to 450 nm, and these spectra tail down to 5% to 10% of peak at 550 nm,[27,59] indicating the feasibility of measuring A2E fluorescence in vivo with excitation wavelengths as long as 550 nm (assuming moderate contributions of other lipofuscin fluorophores[20]). The dominant fluorophore that we measure in vivo exhibits maximum emission at 600 to 640 nm (dependent on excitation wavelength); this peak is expected to shift toward shorter wavelength if ocular media and melanin absorption were fully taken into account. More work needs to be done to eventually reconcile the relationships among the in vivo spectrum, the spectrum of isolated A2E (with the excitation wavelengths used in vivo), and the spectra of intact lipofuscin granules.

Spatial Distribution of Autofluorescence

Our observations confirm previous reports that lipofuscin is lower in the fovea than in the nasal or temporal macula.[2,38] Previous in vivo studies were confounded by the use of short-wavelength excitation, which was partially absorbed by the macular pigment[35,37]; the use in this study of an excitation at 550 nm removes this limitation. Our study provides evidence that fluorescence is not symmetrically distributed around the fovea. In all three sets of measurements (Figs. 3 and 4, Table 3), we found significantly less fluorescence along the inferior meridian than along any other meridian. The distribution of fluorescence in the central 9° around the fovea exhibited large variability (Fig. 3), as was observed in the distribution of lipofuscin in older donor eyes.[6] Asymmetries were also seen as close as 1 to 2° from the fovea (Fig. 5). A limitation of our study is that no measurements were performed outside the meridians, which leaves open the possibility that higher maxima may be located at other sites within quadrants.

Influence of RPE Melanin and Nerve Fiber Layer

We considered whether losses of excitation light and fluorescence through absorption by RPE melanin (discussed above) and/or scattering by the nerve fiber layer could significantly affect the fluorescence distribution and whether regional variation in these entities could explain the observed asymmetries. RPE melanin is greatest at the fovea, decreases substantially from the fovea to approximately 5°, exhibits a broad minimum between 5 and 20°, and then increases slowly toward the

equator.[2,38,53] Using a combination of reflectance and fluorescence measurements,[51] we calculated that the optical density difference in apical melanin between the fovea and 7° from the fovea was effectively 0.10 ± 0.08 DU at 500 nm. For an emission at 650–750 nm (Exc, 550 nm) and using known extinction coefficients for melanin,[53] this corresponds to ≈21% more attenuation of lipofuscin fluorescence at the fovea than at the perifovea. Because we measured foveal levels that are on average 65% of the fluorescence at 7° eccentricity (Table 2), we estimated that the foveal lipofuscin would actually be ≈78% of that at 7° eccentricity. This is consistent with ex vivo measurements[2] that indicated that lipofuscin in the fovea was ≈81% of that at an eccentricity of ≈7°. Thus, the depression in the fluorescence distribution at the fovea (Figs. 3 and 5) is exaggerated as a result of RPE melanin absorption.

The fact that fluorescence at equal eccentricities between 2 and 7° along the horizontal meridians are higher than those along the vertical meridians (Fig. 5) could be explained if greater melanin concentrations occurred superior and inferior to the fovea. However, monochromatic fundus photographs at 570 nm,[60] which delineate higher RPE melanin, are not consistent with such distribution: the area of high RPE melanin is either circular or slightly elongated horizontally. It is difficult to ascertain the role of RPE melanin at larger eccentricities: not only was the spatial resolution of ex vivo measurements of melanin[38,53] too low to account for asymmetries, but information about RPE melanin along the vertical meridians is currently, to our knowledge, unavailable.

Attenuation of light by nerve fibers[61] could also play a role, particularly around the optic disc. However, although there is a 1.5- to 3-fold difference in the thickness of the nerve fiber layer at 7° eccentricity in nasal and temporal meridians,[62,63] there was no marked asymmetry in fluorescence at these sites. Moreover, the thicker nerve fiber observed in the superior retina[62,63] could not explain the reduction of fluorescence observed in the inferior retina. Asymmetries in nerve fiber layer thickness around the fovea may match the observed asymmetries in fluorescence between the horizontal and vertical meridians (at 2–4° eccentricity, Fig. 5): the nerve fiber layer thickens more rapidly along the vertical meridians (lower fluorescence) than along the horizontal meridians (higher fluorescence).[62–64] However, it is unclear how differences in the order of only 5 to 15 μm in nerve fiber layer thickness (at 2–3°) could have the observed effect on the fluorescence. Light loss by scattering by the ganglion cells, whose densities are maximal at 2–3° eccentricity,[65] could not explain the asymmetries because their distribution does not exhibit much asymmetry at those eccentricities.

Because both absorption by melanin[53] and scattering by nerve fibers[61] decrease with increasing wavelength, we assessed, in one subject, whether the distribution obtained with excitation at 470 nm was substantially different from that observed with the 550-nm excitation (Fig. 7). All fluorescences were normalized to the fluorescence at the fovea with excitation at 550 nm. The ratios were drastically lower in the fovea (≈0.3) because of RPE melanin (see above) and macular pigment absorption, but the influence of macular pigment should be negligible by 7° eccentricity.[43] The 470-nm profiles were slightly lower than the 550-nm profiles between 7 and 15° (more so horizontally than vertically), and the ratios were about equal at 20° eccentricity. The plots in Figure 7 argue against a large difference in attenuation by either RPE melanin or nerve fibers at 20° and against a differential attenuation along the superior and inferior meridians. RPE melanin distribution may explain why the differences in fluorescence was stronger along the horizontal meridian than along the vertical meridians.

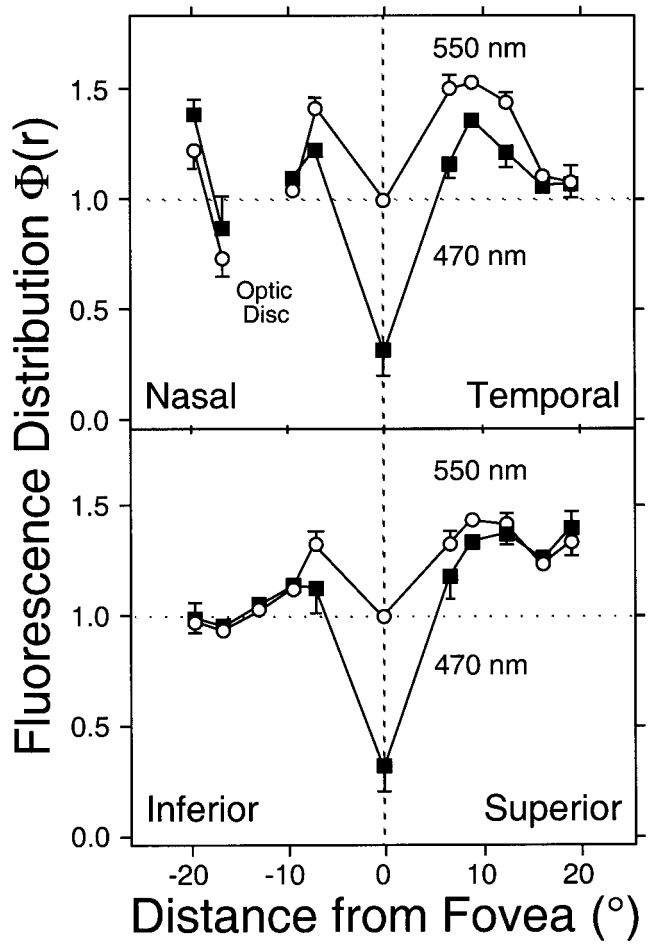

Figure 7. Spatial distribution of autofluorescence along the horizontal (*top*) and vertical (*bottom*) meridians (linear scale) for a 60-year-old subject (same subject as in Fig. 4). The distributions were obtained with excitations at 550 and 470 nm (Em, >650 nm). All 550-nm data were normalized, as before, to the fluorescence at the fovea; the 470-nm data were also normalized to the fluorescence at the fovea with excitation at 550 nm.

Influence of Spatial Distribution of Photoreceptors and Macular Pigment

Because lipofuscin derives from precursors within phagocytosed photoreceptor outer segments, its distribution should reflect that of the photoreceptors.[66] We first compared our fluorescence distribution with the density distribution of rod photoreceptors, as determined by Curcio and colleagues.[41,42] We used Curcio's two age groups[42] that bracket our population: group 1 including ages 27 to 37 years (Fig. 5, curve R1), and group 3 including ages 61 to 75 years (curve R3). For group 1, rod densities are highest in a ring at eccentricities of 10 to 15°, particularly along the superior meridian. Rod densities decrease gradually with age along all meridians.[42] Rod loss is greater at eccentricities of 5 to 12°, inside the ring of highest rod density (gray bars at the top of each panel of Fig. 5). Rod losses are most prominent inferiorly. Maximal rod densities occur at increasing eccentricities with increasing age as the rods in central retina are gradually eroded (Fig. 5).

The distribution of fluorescence roughly matches that of rods at eccentricities larger than 7° (Fig. 5). Maximum fluorescence along each meridian was found inside the ring of highest rod density; the maximum fluorescence occurred at ≈11°, 13°, and 9° from the fovea on the temporal, superior, and inferior

meridian, respectively, whereas the maximum rod densities were at eccentricities of *at least* ≈13°, 14°, and 14°, respectively. At larger eccentricities, rod density decreased less rapidly with increasing eccentricity than fluorescence. Several factors might contribute to both the inward displacement of the fluorescence maxima and the higher slope at high eccentricities. Decreases in the length of the rod outer segment with eccentricity[67,68] and in the rate of rod outer segment renewal,[69] would decrease the volume of the phagosomes and/or reduce the formation of lipofuscin. Light distribution at the posterior pole is unlikely to be a factor.[70]

Our analysis of the age relationship of the inferior–superior difference in fluorescence suggested that the fluorescences were about equal at age 25 and that the fluorescence then increased significantly more slowly inferiorly than superiorly. If premature loss of photoreceptors reduces lipofuscin formation in human as it does in rats,[71,72] then more rapid loss of rods in the inferior retina[42] would reduce, as observed, the rate of lipofuscin accumulation in the inferior retina. Although the areas in which we found greatest lipofuscin accumulation overlap (or are slightly inside) the regions in which the rod loss was greatest (Fig. 5),[42] maximal rod loss did not correspond with the highest fluorescence level at these sites. Indeed, the inferior retina had greater rod loss and lower fluorescence, whereas the superior retina had lower rod loss and higher fluorescence. These considerations suggest that the age-related loss of rods cannot be predicted by lipofuscin accumulation, confirming the conclusions of Curcio et al.,[42] which were based on an alternate rationale.

In the central area, lipofuscin fluorescence exhibits a shallow minimum (Fig. 3) that is slightly displaced in the nasal-inferior direction by an average of 0.5°. This zone on minimal fluorescence overlaps the rod-free zone, which is also slightly displaced nasally.[41] Isofluorescence contours are slightly elliptical with a long vertical axis, in contrast to rods and cones whose isodensity contours are horizontally oriented ellipses.[41] Cone density is maximal in the fovea (where the density exceeds the maximal density of rods) and decreases rapidly with eccentricity: by 3.0 to 3.5° cone density is only 10% of its maximum (Fig. 5).[41] The narrowness of the cone distributions makes it impossible to reconcile the fluorescence distribution with any simple linear combination of cone and rod density distributions. The fluorescence distribution in the foveal area may also be influenced by RPE melanin distribution (mentioned above), macular pigment (discussed below), and by numerous other factors such as the variation with eccentricity of cone types, outer segment length, rate of outer segment renewal,[69] and rate of lipofuscin formation in the RPE. Rod/cone differences in some of these factors will also influence the relative contributions of each photoreceptor type to the formation of lipofuscin. Anderson and colleagues[73] found in Rhesus monkeys that the number of foveal (cone-derived) phagosomes in the RPE was only one third of the number of extrafoveal phagosomes (mainly rod derived), suggesting that the rate of lipofuscin formation associated with cones may be slower.

Macular pigment (lutein and zeaxanthin in cone axons) reaches peak optical densities of up to 1.0 DU (at 460 nm) in the fovea, and its density distribution is symmetrical and very similar to that of cones.[43] Because it absorbs blue light, macular pigment may substantially reduce blue-light–activated mechanisms of lipofuscin and A2E formation (see Introduction). However, as in case of the cone distribution, the distribution of macular pigment is also very narrow; it reaches 10% of its peak density at 3.1 ± 1.3°.[43] The depression in lipofuscin fluorescence observed within eccentricities of ≈8° is thus much larger than the area occupied by the densest macular pigment, and a simple protective effect of the macular pigment is thus not observed in the spatial distribution. However, approximately 70% of the total retinal lutein and zeaxanthin is contained within the rod outer segments,[74] where they may act as antioxidants,[75] slowing the rate of lipofuscin formation.[76,77] The lutein and zeaxanthin within the outer segments also declines with increasing eccentricity, which could account for part of the gradual increase in fluorescence with eccentricity. Combined measurements of the spatial density distribution of the macular pigment[51] and lipofuscin in individuals, and a better understanding of the physiology of the lutein and zeaxanthin in rods and cones will help resolve to what extent their distribution controls that of lipofuscin.

The data presented here indicate that the distribution of lipofuscin reflects, rather than predicts, the age-related loss of photoreceptors. However, excessive accumulation of lipofuscin may contribute to the etiology of photoreceptor atrophy in Stargardt's macular dystrophy and possibly AMD. Bull's-eye regions of atrophy in a variety of retinal diseases, including AMD and Stargardt's disease, have been attributed to the protective effect of the macular pigment and the ring-like region of high lipofuscin.[78] In age-related maculopathy, the distribution of soft indistinct drusen and pigmentary abnormalities outside the central area[44] roughly matches that of lipofuscin: they were more prevalent in the superior retina (where lipofuscin fluorescence is higher) than they were in the inferior retina (where lipofuscin in always lower). However, soft indistinct drusen and pigmentary abnormalities were most prevalent in the central 3° diameter region (where lipofuscin is ≈80% of maximal). Clearly, lipofuscin could only be one of the multiple factors influencing susceptibility to retinal damage. Understanding the cause and nature of the focal and global distribution in lipofuscin fluorescence may advance the understanding of the pathogenesis of AMD. Lipofuscin measurement may ultimately prove an excellent screening tool to recognize subjects at high risk for AMD and other maculopathies, and/or to evaluate new therapies targeting accumulation and/or liberation of A2E. To further elucidate the relationship of lipofuscin and retinal pathology, it will be necessary to obtain the distributions of fluorescence and pathology in subjects with age-related maculopathy and in patients with early AMD.

Acknowledgments

The authors express their gratitude to Christine Curcio (University of Alabama, Birmingham, AL) for graciously supplying the numerical data on rod photoreceptor distributions.

References

1. Feeney-Burns L, Hilderbrand ES, Eldridge S. Aging human RPE: morphometric analysis of macular, equatorial, and peripheral cells. *Invest Ophthalmol Vis Sci.* 1984;25:195–200.
2. Weiter JJ, Delori FC, Wing G, Fitch KA. Retinal pigment epithelial lipofuscin and melanin and choroidal melanin in human eyes. *Invest Ophthalmol Vis Sci.* 1986;27:145–152.
3. Young RW. Pathophysiology of age-related macular degeneration. *Surv Ophthalmol.* 1987;31:291–306.
4. Eldred GE. Questioning the nature of the fluorophores in age pigments. *Adv Biosci.* 1987;64:23–36.
5. Taylor A, Jacques PF, Dorey CK. Oxidation and aging: impact on vision. *J Toxicol Indust Health.* 1993;9:349–371.
6. Dorey CK, Staurenghi G, Delori FC. Lipofuscin in aged and AMD eyes. In: Holyfield JG, Anderson RE, LaVail MMs, eds. *Retinal Degeneration*. New York: Plenum Press; 1993:3–14.
7. Holz FG, Bellmann C, Margaritidis M, Schutt F, Otto TP, Volcker HE. Patterns of increased in vivo fundus autofluorescence in the junctional zone of geographic atrophy of the retinal pigment

epithelium associated with age-related macular degeneration. *Graefes Arch Clin Exp Ophthalmol.* 1999;237:145–152.
8. Eagle RC, Lucier AC, Bernadino VB, Janoff M. Retinal pigment epithelial abnormalities in fundus flavimaculatus: a light and electron microscopic study. *Ophthalmology.* 1980;87:1189–1200.
9. Allikmets R, Singh N, Sun H, et al. A photoreceptor cell-specific ATP-binding transporter gene (*ABCR*) is mutated in recessive Stargardt macular dystrophy. *Nat Genet.* 1997;15:236–245.
10. Azarian SM, Travis GH. The photoreceptor rim protein is an ABC transporter encoded by the gene for recessive Stargardt's disease (ABCR). *FEBS Lett.* 1997;409:247–252.
11. Molday LL, Rabin AR, Molday RS. ABCR expression in foveal cone photoreceptors and its role in Stargardt macular dystrophy. *Nat Genet.* 2000;25:257–258.
12. Delori FC, Staurenghi G, Arend O, Dorey CK, Goger DG, Weiter JJ. In vivo measurement of lipofuscin in Stargardt's disease/Fundus flavimaculatus. *Invest Ophthalmol Vis Sci.* 1995;36:2331–2337.
13. von Rückmann A, Fitzke FW, Bird AC. In vivo fundus autofluorescence in macular dystrophies. *Arch Ophthalmol.* 1997;115:609–615.
14. Weng J, Mata NL, Azarian SM, Tzekov RT, Birch DG, Travis GH. Insights into the function of Rim protein in photoreceptors and etiology of Stargardt's disease from the phenotype in abcr knockout mice. *Cell.* 1999;98:13–23.
15. Kramer F, White K, Pauleikhoff D, et al. Mutations in the VMD2 gene are associated with juvenile-onset vitelliform macular dystrophy (Best disease) and adult vitelliform macular dystrophy but not age-related macular degeneration. *Eur J Hum Genet.* 2000;8:286–292.
16. Armstrong D, Koppang N, Rider J. *Ceroid lipofuscinsosis (Battens Disease).* Amsterdam: Elsevier; 1982.
17. Boulton M, Dontsov A, Jarvis-Evans J, Ostrovsky M, Svistunenko D. Lipofuscin is a photoinducible free radical generator. *J Photochem Photobiol B.* 1993;19:201–204.
18. Gaillard RR, Atherton SJ, Eldred G, Dillon J. Photophysical studies on human retinal lipofuscin. *Photochem Photobiol.* 1995;61:448–453.
19. Rozanowska M, Jarvis-Evans J, Korytowski W, Boulton ME, Burke JM, Sarna T. Blue light-induced reactivity of retinal age pigment. In vitro generation of oxygen-reactive species. *J Biol Chem.* 1995;270:18825–18830.
20. Eldred GE, Katz ML. Fluorophores of the human retinal pigment epithelium: separation and spectral characterization. *Exp Eye Res.* 1988;47:71–86.
21. Eldred CE, Laskey MR. Retinal age pigments generated by self-absorbing lysosomotropic detergents. *Nature.* 1993;361:724–726.
22. Sakai N, Decatur J, Nakanishi K, Eldred GE. Ocular age pigment "A2-E": an unprecedented pyridinium bisretinoid. *J Am Chem Soc.* 1996;118:1559–1560.
23. Liu J, Itagaki Y, Ben-Shabat S, Nakanishi K, Sparrow JR. The biosynthesis of A2E, a fluorophore of aging retina, involves the formation of the precursor, A2-PE, in the photoreceptor outer segment membrane. *J Biol Chem.* 2000;275:29354–29360.
24. Mata NL, Weng J, Travis GH. Biosynthesis of a major lipofuscin fluorophore in mice and humans with ABCR-mediated retinal and macular degeneration. *Proc Natl Acad Sci USA.* 2000;97:7154–7159.
25. Holz FG, Schutt F, Kopitz J, et al. Inhibition of lysosomal degradative functions in RPE cells by a retinoid component of lipofuscin. *Invest Ophthalmol Vis Sci.* 1999;40:737–743.
26. Schutt F, Davies S, Kopitz J, Holz FG, Boulton ME. Photodamage to human RPE cells by A2-E, a retinoid component of lipofuscin. *Invest Ophthalmol Vis Sci.* 2000;41:2303–2308.
27. Sparrow JR, Nakanishi K, Parish CA. The lipofuscin fluorophore A2E mediates blue light-induced damage to retinal pigmented epithelial cells. *Invest Ophthalmol Vis Sci.* 2000;41:1981–1989.
28. Tamagaki C, Murata A, Asai S, et al. Age-related changes of cornu ammonis 1 pyramidal neurons in gerbil transient ischemia [In Process Citation]. *Neuropathology.* 2000;20:221–227.
29. Nakanishi H, Amano T, Sastradipura DF, et al. Increased expression of cathepsins E and D in neurons of the aged rat brain and their colocalization with lipofuscin and carboxy-terminal fragments of Alzheimer amyloid precursor protein. *J Neurochem.* 1997;68:739–749.
30. Sparrow JR, Parish CA, Hashimoto M, Nakanishi K. A2E, a lipofuscin fluorophore, in human retinal pigmented epithelial cells in culture. *Invest Ophthalmol Vis Sci.* 1999;40:2988–2995.
31. Suter M, Reme CE, Grimm C, et al. Age-related macular degeneration: the lipofuscin component *N*-Retinyl-*N*-Retinylidene detaches proapoptotic proteins from mitochondria and induces apoptosis in mammalian retinal pigment epithelial cells. *J Biol Chem.* 2000;275:39625–39630.
32. Bensaoula T, Shibuya H, Katz ML, et al. Histopathologic and immunocytochemical analysis of the retina and ocular tissues in Batten disease. *Ophthalmology.* 2000;107:1746–1753.
33. Delori FC. RPE lipofuscin in aging and age related macular degeneration. In: Piccolino FC, and Coscas G, eds. *Retinal Pigment Epithelium and Macular Diseases*. Dordrecht, The Netherlands: Kluwer Academic Publishers; 1998:37–45.
34. Delori FC. Spectrophotometer for noninvasive measurement of intrinsic fluorescence and reflectance of the ocular fundus. *Applied Optics.* 1994;33:7439–7452.
35. von Rückmann A, Fitzke FW, Bird AC. Distribution of fundus autofluorescence with a scanning laser ophthalmoscope. *Br J Ophthalmol.* 1995;119:543–562.
36. Delori FC, Fleckner MR, Goger DG, Weiter JJ, Dorey CK. Autofluorescence distribution associated with drusen in age-related macular degeneration. *Invest Ophthalmol Vis Sci.* 2000;41:496–504.
37. Delori FC, Dorey CK, Staurenghi G, Arend O, Goger DG, Weiter JJ. In vivo fluorescence of the ocular fundus exhibits retinal pigment epithelium lipofuscin characteristics. *Invest Ophthalmol Vis Sci.* 1995;36:718–729.
38. Wing GL, Blanchard GC, Weiter JJ. The topography and age relationship of lipofuscin concentration in the retinal pigment epithelium. *Invest Ophthalmol Vis Sci.* 1978;17:601–607.
39. Okubo A, Rosa RH Jr, Bunce CV, et al. The relationships of age changes in retinal pigment epithelium and Bruch's membrane. *Invest Ophthalmol Vis Sci.* 1999;40:443–449.
40. von Rückmann A, Fitzke FW, Bird AC. Fundus autofluorescence in age-related macular disease imaged with a laser scanning ophthalmoscope. *Invest Ophthalmol Vis Sci.* 1997;38:478–486.
41. Curcio CA, Sloan KR, Kalina RE, Hendrickson AE. Human photoreceptor topography. *J Comp Neurol.* 1990;292:497–523.
42. Curcio CA, Millican CL, Allen KA, Kalina RE. Aging of the human photoreceptor mosaic: evidence for selective vulnerability of rods in central retina. *Invest Ophthalmol Vis Sci.* 1993;34:3278–3296.
43. Hammond BR Jr, Wooten BR, Snodderly DM. Individual variations in the spatial profile of human macular pigment. *J Opt Soc Am A.* 1997;14:1187–1196.
44. Wang Q, Chappell RJ, Klein R, et al. Pattern of age-related maculopathy in the macular area. *The Beaver Dam Eye Study. Invest Ophthalmol Vis Sci.* 1996;37:2234–2242.
45. Bird AC, Bressler NM, Bressler SB, et al. An international classification and grading system for age-related maculopathy and age-related macular degeneration (The International ARM Epidemiological Study Group). *Surv Ophthamol.* 1995;39:367–374.
46. Delori FC, Burns SA. Fundus reflectance and the measurement of crystalline lens density. *J Opt Soc Am A.* 1996;13:215–226.
47. Delori FC, Dorey CK. In vivo technique for autofluorescent lipopigments. In: Armstrong DS, eds. *Methods in Molecular Biology, Vol. 108: Free Radicals and Antioxidant Protocols*. Totowa: Humana Press; 1998:229–243.
48. Wyszecki G, Stiles WS. *Color Science: Concepts and Methods, Quantitative Data and Formulae*. New York: John Wiley & Sons; 1982.
49. Pokorny J, Smith VC, Lutze M. Aging of the human lens. *Appl Opt.* 1987;26:1437–1440.
50. Weale RA. Age and the transmittance of the human crystalline lens. *J Physiol.* 1988;395:577–587.
51. Delori F, Goger D, Hammond B, Snodderly D, Burns S. Macular pigment density measured by autofluorescence spectrometry: comparison with reflectometry and heterochromatic flicker photometry. *J Opt Soc Am A.* In press.

52. Bone RA, Landrum JT, Cains A. Optical density spectra of the macular pigment in vivo and in vitro. *Vision Res.* 1992;32:105–110.
53. Gabel V-P, Birngruber R, Hillenkamp F. Visible and near infrared light absorption in pigment epithelium and choroid. In: Shimuzu K, Osterhuis JAS, eds. *XXIII Concilium Ophthalmol Kyoto.* Amsterdam-Oxford: Exerpta Medica; 1978:658–662.
54. Boulton MD, Dayhaw-Barker F, Ramponi P, Cubeddu R. Age-related changes in the morphology, absorption and fluorescence of melanosomes and lipofuscin granules of the retinal pigment epithelium. *Vision Res.* 1990;30:1291–1303.
55. Schmidt SY, Peisch RD. Melanin concentration in normal human retinal pigment epithelium: regional variation and age-related reduction. *Invest Ophthalmol Vis Sci.* 1986;27:1063–1067.
56. Feeney-Burns L, Berman ER, Rothman H. Lipofuscin of human retinal pigment epithelium. *Am J Ophthalmol.* 1980;90:783–791.
57. Gao H, Hollyfield JG. Aging of the human retina: differential loss of neurons and retinal pigment epithelial cells. *Invest Ophthamol Vis Sci.* 1992;33:1–17.
58. Arend OA, Weiter JJ, Goger DG, Delori FC. In-vivo fundus-fluoreszenz-messungen bei patienten mit alterabhangiger makulardegeneration. *Ophthalmologie.* 1995;92:647–653.
59. Parish CA, Hashimoto M, Nakanishi K, Dillon J, Sparrow J. Isolation and one-step preparation of A2E and iso-A2E, fluorophores from human retinal pigment epithelium. *Proc Natl Acad Sci USA.* 1998; 95:14609–14613.
60. Delori FC, Gragoudas ES, Francisco R, Pruett RC. Monochromatic ophthalmoscopy and fundus photography: the normal fundus. *Arch Ophthalmol.* 1977;95:861–868.
61. Knighton RW, Jacobson SG, Kemp CM. The spectral reflectance of the nerve fiber layer of the macaque retina. *Invest Ophthalmol Vis Sci.* 1989;30:2393–2402.
62. Radius RL. Thickness of the retinal nerve fiber layer in primate eyes. *Arch Ophthalmol.* 1980;98:1625–1629.
63. Ogden TE. Nerve fiber layer of the primate retina: thickness and glial content. *Vision Res.* 1983;23:581–587.
64. Varma R, Skaf M, Barron E. Retinal nerve fiber layer thickness in normal human eyes [published erratum appears in *Ophthalmology* Feb;104:174]. *Ophthalmology.* 1996;1997:103:2114–2119.
65. Curcio CA, Allen KA. Topography of ganglion cells in human retina. *J Comp Neurol.* 1990;300:5–25.
66. Feeney-Burns L, Eldred CE. The fate of the phagosome: conversion to "age pigment" and impact in human retinal pigment epithelium. *Trans Ophthal Soc UK.* 1983;103:416–421.
67. Hendrickson A, Drucker D. The development of parafoveal and mid-peripheral human retina. *Behav Brain Res.* 1992;49:21–31.
68. Dorn EM, Hendrickson L, Hendrickson AE. The appearance of rod opsin during monkey retinal development. *Invest Ophthalmol Vis Sci.* 1995;36:2634–2651.
69. Young RW. Biological renewal. Application to the eye. *Trans Ophthalmol Soc UK.* 1982;102:42–75.
70. Pflibsen KP, Pomerantzeff O, Ross RN. Retinal illuminance using a wide-angle model of the eye. *J Opt Soc Am.* 1988;5:146–150.
71. Katz ML, Drea CM, Eldred GE, Hess HH, Robison WG Jr. Influence of early photoreceptor degeneration on lipofuscin in the retinal pigment epithelium. *Exp Eye Res.* 1986;43:561–573.
72. Katz ML, Eldred GE. Retinal light damage reduces autofluorescent pigment deposition in the retinal pigment epithelium. *Invest Ophthalmol Vis Sci.* 1989;30:37–43.
73. Anderson DH, Fisher SK, Erickson PA, Tabor GA. Rod and cone disc shedding in the rhesus monkey retina: a quantitative study. *Exp Eye Res.* 1980;30:559–574.
74. Rapp LM, Maple SS, Choi JH. Lutein and zeaxanthin concentrations in rod outer segment membranes from perifoveal and peripheral human retina. *Invest Ophthalmol Vis Sci.* 2000;41:1200–1209.
75. Sujak A, Gabrielska J, Grudzinski W, Borc R, Mazurek P, Gruszecki WI. Lutein and zeaxanthin as protectors of lipid membranes against oxidative damage: the structural aspects. *Arch Biochem Biophys.* 1999;371:301–307.
76. Katz ML, Stone W, Dratz EA. Fluorescent pigment accumulation in RPE of antioxidant deficient rats. *Invest Ophthalmol Vis Sci.* 1978; 17:1049–1058.
77. Terman A, Brunk UT. Lipofuscin: mechanisms of formation and increase with age. *Apmis.* 1998;106:265–276.
78. Weiter JJ, Delori FC, Dorey CK. Central sparing in annular macular degeneration. *Am J Ophthalmol.* 1988;106:286–292.